Korean J. Chem. Eng., **27**(5), 1606-1612 (2010)
DOI: 10.1007/s11814-010-0240-5

Attrition behavior of fine particles in a fluidized bed with bimodal particles: Influence of particle density and size ratio

Zeeshan Nawaz†, Tang Xiaoping, Xiaobo Wei, and Fei Wei

Beijing Key Laboratory of Green Chemical Reaction Engineering and Technology (FLOTU), Department of Chemical Engineering, Tsinghua University, Beijing 100084, China
(*Received 30 September 2009 • accepted 31 December 2009*)

Abstract−To process the solid particulates in fluidized bed and slurry phase reactors, attrition is an inevitable consequence and is therefore one of the preliminary parameters for the catalyst design. In this paper, the mechanical degradation propensity of the zeolite catalysts (particles) was investigated in a bimodal distribution environment using a Gas Jet Attrition - ASTM standard fluidized bed test (D-5757). The experimentation was conducted in order to explore parameters affecting attrition phenomena in a bimodal fluidization. In a bimodal fluidization system, two different types of particles are co-fluidized isothermally. The air jet attrition index (AJI) showed distinct increases in the attrition rate of small particles in a bimodal fluidization environment under standard operating conditions, in comparison with single particle. A series of experiments were conducted using particles of various sizes, with large particles of different densities and sizes. Experimental results suggest that the relative density and particle size ratio have a significant influence on attrition behavior during co-fluidization. Therefore a generalized relationship has been drawn using Gwyn constants; those defined material properties of small particles. Moreover, distinct attrition incremental phenomenon was observed during co-fluidization owing to the change in collision pattern and impact, which was associated with relative particle density and size ratios.

Key words: Attrition, Zeolite Catalysts, Co-fluidization, Fracture, Abrasion

INTRODUCTION

It has long been known that particle attrition is an unavoidable phenomenon in fluidization. Therefore, fluidized bed processes have fines recovery systems (e.g. cyclones); however, high attrition resistant catalysts have been preferred. In general, attrition is the segregation and fractionation of solid particles [1]. This undesired breakdown of solid particles frequently encountered problems in reactors, especially with changing flow regimes [2], such as loss of catalyst, pipe/wall abrasion, changes in bulk properties [3], stack opacity [3], and a decrease in the quality of product due to separation problems [4]. In general, attrition resistance was affected by several intrinsic properties of the particles (size distribution, shape, porosity, surface, cracks, electrostatic charge generation, hardness of the particles, etc.) and the operational environment (exposure time, shear, gas velocity, bed length, movement, collision, impact, pressure, temperature, etc.) [1,5].

Several experimental studies and empirical models were developed in order to characterize the extent of attrition in a fluidized environment. Gwyn et al. [6] developed the following empirical relationship (see Eq. (1)) by considering shearing time of attrition, using a single particle system with high velocity air jets in a fluidized bed. However, particulate attrition indices considering single-particle impact provide an ambiguous picture as Gwyn did not consider principal affecting parameters. The Gwyn constants K and m, were the function of material properties and size, and were determined experimentally; further details can be found elsewhere [6].

$$W=Kt^m \tag{1}$$

Many other studies have discussed attrition and the deformation of particles, or breakage phenomenon using various shapes, materials (e.g., urea prills, TAED, sodium chloride, molecular sieve beads, heavy soda ash and alumina extrudates) and systems (e.g., shear cell, annular cell, phunamatic convares, fluidized beds, etc.) [7-10]. The size distribution of generated fines as a result of attrition was previously defined by Schuhmann [7]. Neil and Bridgwater employed the Gwyn equation to characterize different particulate systems--fluidized bed, screw pugmill, and annular shear cell--and found that one of the characteristic parameters of the Gwyn function, m, is independent of the equipment type [10]. Moreover, Neil and Bridgwater proposed that m is a constant for a given material and the constant of proportionality, K, was related to the normal stress. Crutchley and Bridgwater measured the gap size influence on particle attrition in cone cell and observed a maximum attrition rate at gap widths of approximately two particle diameters [11]. Ghadiri et al. focused on fragmentation and surface damaging phenomena on the basis of load and strain [12]. Potapov and Campbell studied particle breakage induced mechanisms [13]. Consequently, Ghadiri and Zhang developed a relationship (see Eq. (2)) for the fractional loss of particles due to impact [14].

$$\xi=\alpha\eta=\alpha(\rho v^2 l H/K_c^2) \tag{2}$$

However, to date, no study has focused on particle attrition phenomena in bimodal particle fluidized bed (co-fluidization environments), i.e., the most feasible design for handling extremely endo-

†To whom correspondence should be addressed.
E-mail: zeeshan@mails.tsinghua.edu.cn

thermic or exothermic reactions, while the disadvantage of attrition [15] becomes serious. Therefore, the present study focused attention not only on attrition calculations, but explored its incremental phenomena and developed a more generalized relationship for calculating attrition debris in a bi-modal particle system. The Gas Jet Attrition - ASTM standard fluidized bed test method (D-5757-Revised) was used for determining attrition resistance of catalyst particles, and was calculated in terms of Air Jet Index (percentage loss) [16].

EXPERIMENTAL

1. Materials

ZSM-5 and SAPO-34 zeolites of two different sizes, 0.098 mm and 0.15 mm, were used as small particles. The SAPO-34 catalyst was prepared at the Beijing Key Laboratory of Green Chemical Reaction Engineering, Tsinghua University, Beijing, with the mixture composition: SAPO-34 zeolite, kaolin and silicon solution with a weight ratio of 30%, 40% and 30%, respectively. Both ZSM-5 and SAPO-34 small-sized particles have density 1.68 g/cm^3. The large and small ZSM-5 particles of 2.7 mm were provided by Hui Er San Ji Co., Ltd. Beijing, China. Large ceramic balls of 0.7 mm having composition $Al_2O_3/ZrO_2/SiO_2$, with 40/10/50 weight percent respectively, were used. And large hollow ceramic balls of 0.7 mm and 1.2 mm were manufactured by Gongyi SanYuan Ceramic Co., Ltd. China. The small-sized particles and fines were characterized using a Malvern Mastersizer (MICRO-PLUS). The sizes of the large particles were measured with a Vernier caliper. Particle morphology was obtained (before and after the attrition experiment) by using a JEOL JSM 7401F scanning electron microscope (SEM) at an accelerating voltage of 3.0 kV.

2. Gas Jet Attrition Test (ASTM Standard Fluidized Method)

The attrition behaviors of particles were investigated using a gas jet attrition apparatus. This unit was designed based on a standard ASTM D-5757 (Revised) test method [16]. Induced particle breakage mechanisms in air-jet tests were believed to involve fractures (in the grid region of the apparatus) and abrasions (in the bubble zone of the apparatus) [5]. All tests were conducted with nitrogen at room temperature. An operating procedure was followed that included gas velocity beyond that of the terminal velocity for a given particle size range allowed in D-5757. It allows the fine particles (>50 μm) to transport to a fine collection chamber. 25.0 g large and 25.0 g small particles were loaded into an attrition tube, and the gas flow rate was adjusted gradually at 0.60 m^3/hr (0.059 m/s) according to the ASTM standard D-5757. The gas jet attrition apparatus is shown in Fig. 1 and its design features were as follows:

(a) A stainless steel 70 cm long attrition tube of OD 12 cm.
(b) Three nozzles of diameter 0.38 mm, equidistant from each other, 10 mm from center.
(c) Settling chamber, 62 cm long cylinder of inner diameter 34 cm with conical ends.
(d) Fines collection assembly, filtering the fines from the gas.

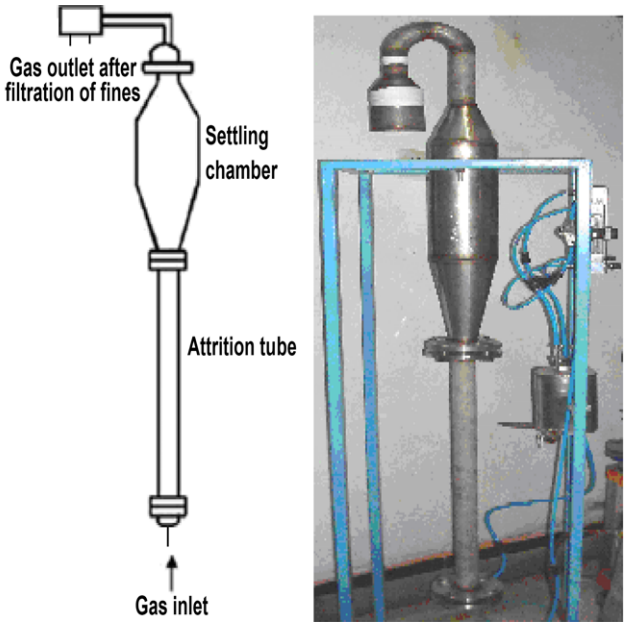

Fig. 1. Gas Jet Attrition experimental rig.

RESULTS AND DISCUSSION

The Air Jet Index (AJI) of all samples was calculated from the elutriated fines collected after a series of experimental runs. The

Table 1. Gas Jet Attrition Index and Gwyn constants for single particle systems

Exp. no.	Run	Material	Particle size, mm	AJI after 5 h	K	m
1	I	ZSM-5	0.098	0.0028	0.0987	0.4339
	II	ZSM-5	0.098	0.003	0.0987	0.4339
2	I	ZSM-5	0.15	0.0026	0.0653	0.4321
	II	ZSM-5	0.15	0.0026	0.0653	0.4321
3	I	SAPO-34	0.098	0.0082	0.2027	0.4513
	II	SAPO-34	0.098	0.008	0.2027	0.4513
4	I	SAPO-34	0.15	0.0052	0.1254	0.4348
	II	SAPO-34	0.15	0.0052	0.1254	0.4348
5	I	Ceramic Balls	0.7	0	0	0
6	I	Hollow Ceramic Balls	0.7	0	0	0
7	I	Hollow Ceramic Balls	1.2	0	0	0
8	I	ZSM-5	2.7	0	0	0

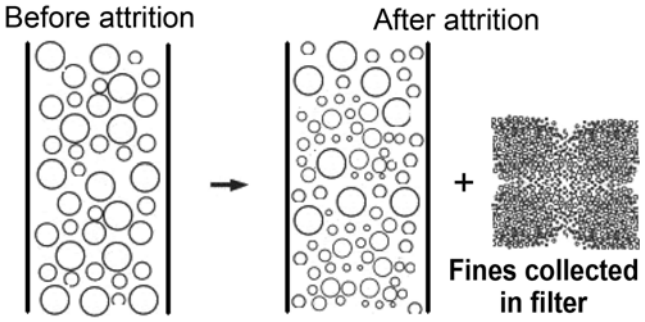

Fig. 2. Systematic image of attrition tube before and after attrition run.

negligible loss of particles (catalyst) associated with disassembly of the attrition tube was noted, and the overall recoveries were about 99% in each experimental run. The overall weight loss was used as fine particles losses during calculations. AJI demonstrates overall attrition debris and Gwyn constants were tabulated for single particle system (see Table 1). Based on the above analysis, the particles can be classified into two generalized groups elutriated (fines collected from filter having size smaller than 50 μm) and un-elutriated particles (those retained in attrition tube) according to their original particle size and system was systematically shown in Fig. 2. The Gwyn constants K and m, those were the function of material properties and size [6], were experimentally determined for each small particle in a single particle fluidization system (for both SAPO-34 and ZSM-5 of particle size 0.098 mm and 0.15 mm). The catalyst showed good resistance to attrition, with the maximum AJI value of 0.004, meaning that just 0.40% of the initial sample was lost or converted into fines in 5 hr. The observed attrition rate was almost linear. The attrition of coarse particles of varying densities and sizes showed excellent resistance to attrition, with an AJI value of zero, which means that 100% of the sample was recovered after 5 hr.

The main objective behind current experimentation was to analyze the variations in small particle attrition during bimodal fluidization (gas-solid-solid) system and to explore the influence of relative density and particle size ratio on attrition behavior. As in the GSS-CFR (gas-solid-solid circulating fluidized bed), two solid particles were prone to be co-fluidized, and the attrition behavior was largely varied from single particle attrition. AJI in certain cases was as high as 0.28, which means that 28% of the small particles were lost due to attrition. The attrition evaluation was generally pronounced by the attrition rate, which depends upon certain threshhold for the size limit of fines collected. In practice, attrition mass was more important than the collected fine's size distribution; therefore, ASTM standard D-5757 attrition test method was selected for the present study and operated under standard operating procedure, in the density range of 1-3 g/cm^3 [16].

The flow regime changes with density variations and fluidization velocities, but the settling chamber provides slipping area to keep the particles airborne in these circumstances, and only lets the fines go out. Therefore, the ASTM standard fluidized bed was selected and operated at fixed superficial gas velocity, i.e., 0.059 m/s, according to the standard operating procedure. The exact values of Gwyn constants for each particle (small zeolite catalysts) at standard conditions were evaluated in accordance with an exact protocol. Later

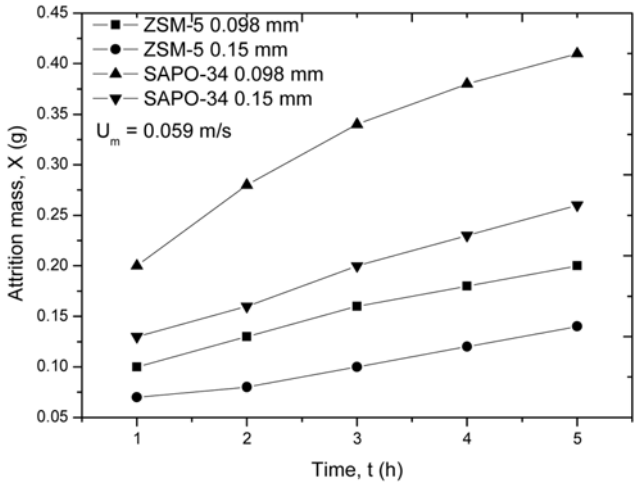

Fig. 3. Single particle system Gwyn plot for attrition debris of zeolite catalyst particles.

the co-fluidization tests were carried out at same conditions using the same apparatus in order to avoid ambiguity regarding operational influences. The Gwyn constants of each small particle were measured experimentally as shown in Table 1. The Gwyn plots for the single particle system, i.e., the results of overall attrition mass generated by different samples, are shown in Fig. 3. A linear relationship was found between attrition mass generated against designated time. This model does not have the ability to be extrapolated to a bi-modal system; moreover, severe deviations appear in certain single particle systems [17]. To avoid this error, we calculated Gwyn constants of our material online in a similar apparatus, so that their formulation errors regarding different equipment did not appear.

In general, the Gwyn formulation was more successful in describing attrition of single-sized particles, as discussed earlier, and widely deviated in apparent circumstances [17]. The severe deviation of the Gwyn empirical relationship is shown in Fig. 4, i.e., the case of a bimodal particle fluidization system, having particles of two different sizes and densities. Cohesive forces developed by large particles were also large in comparison with small-sized particles. This leads to larger collision impact and increases attrition rate. To avoid this ambiguity in the analysis of attrition debris generated in gas-solid-solid fluidization, we formulated a new relationship based on the standard operation data, using Gwyn constants for small particles (calculated in single particle system) and by considering the densities and size ratios for large particles. Previously, Neil et al. [10] asserted that the Gwyn constant m was independent of loading rate, the type of equipment used and systems employed. While large deviations were noted in the present experimentation, a new relationship was proposed that explains this situation in a well defined manner (see Eq. (4)). Where Z represents the severity of attrition due to size variation and relative density (dimensionless), while e accounts for the change in material properties with time; and where K and m were the Gwyn parameters related to the properties of small particles [6,10].

The effect of relative density was considered to define this new constant Z and its influence can be observed in Fig. 5. There it is assumed that S is constant and its value is 1. This newly developed function (Eq. (4)) has the ability to successfully explain small particle

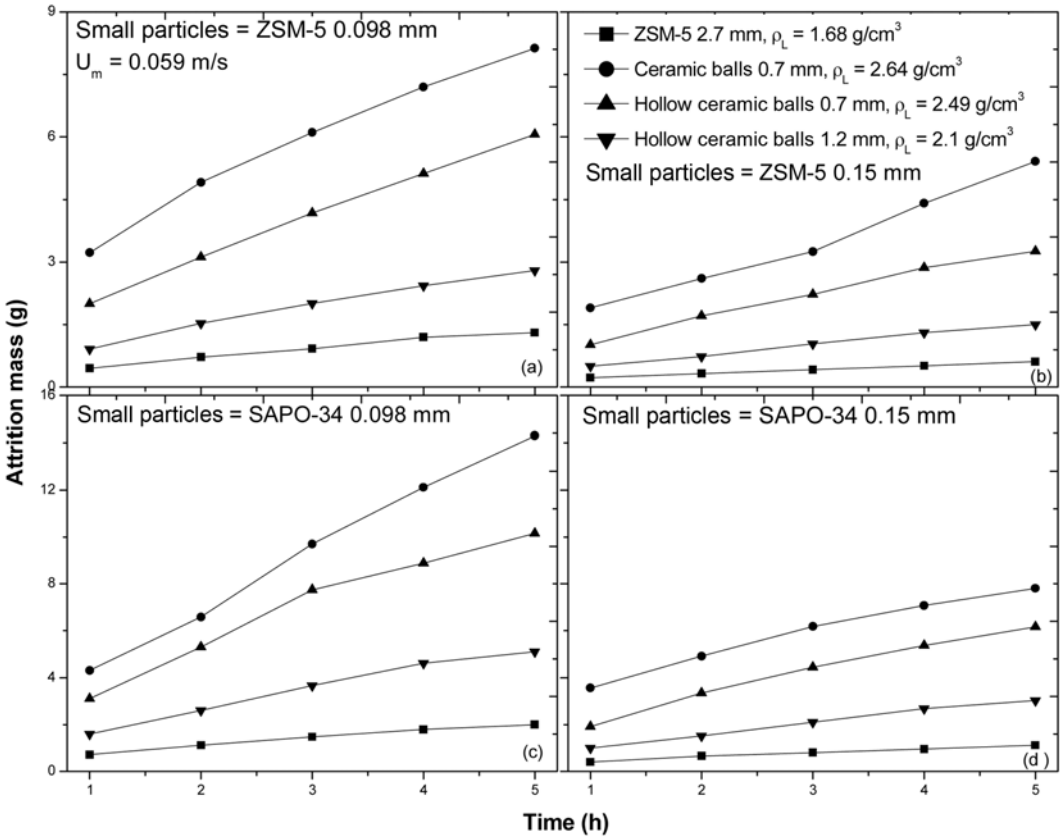

Fig. 4. Attrition behavior in two particle system (GSS) of different density and sized large particles on (a) small zeolite ZSM-5 0.098 mm particles (b) small zeolite ZSM-5 0.15 mm particles (c) small zeolite SAPO-34 0.098 mm particles (d) small zeolite SAPO-34 0.15 mm particles.

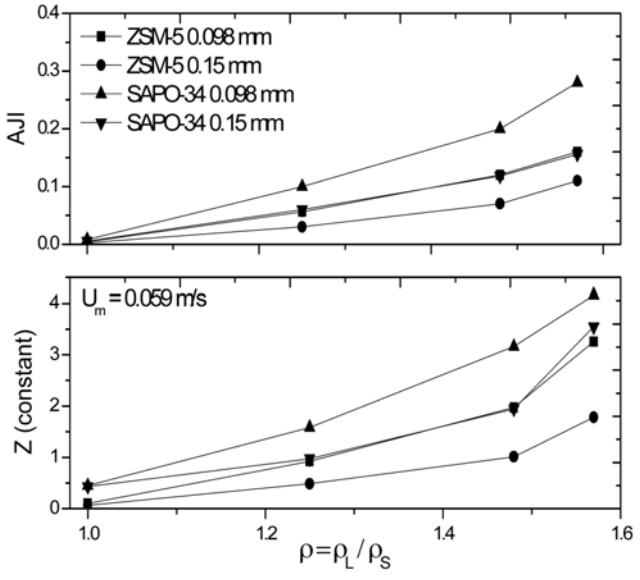

Fig. 5. Effect of relative density on newly defined constant Z and AJI after 5 hr.

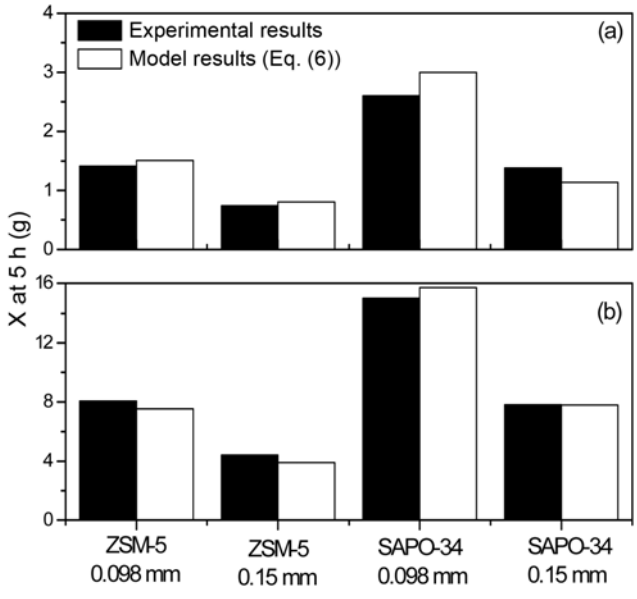

Fig. 6. Comparison of Zeeshan formulation and experimental results over a wide range (a) co-fluidized with ZSM-5 particles of density 1.68 g/cm^3 and 2.7 mm size, (b) co-fluidized with high density ceramic balls 2.64 g/cm^3 and 0.7 mm size.

attrition of zeolites and other synthetic catalysts used in bimodal fluidized bed reactors. This empirical relationship will become more generalized and accurate because Gwyn constants of each particle (catalyst) were determined individually. Therefore, the applicability of this function is not only limited to the measurement of zeolites attrition in a bimodal fluidized bed environment but can be used

for other catalysts. The proposed relationship simulated results were compared over a wide range of experimental results and shown in Fig. 6. Furthermore, in defining this new function, we consider the impact of large particles as a function of relative density and particle size ratio. Moreover, it was assumed that there is no loss of large particles (as observed from their subsequent single particle experimental data). A narrow span of deviation, i.e., ±0.50 g, in attrition debris after 5.0 hours operation was observed. The model was generalized as changes related to material properties, and by considering these properties the relationship was made generalized. For each type of material we first determine the values of their constants for a single particle system as explained by Gwyn, and then using proposed model the attrition loss of that sample in a bi-modal fluidization at designated conditions can be calculated.

$$x=Z\cdot t^{e} \quad (3)$$

where

$$Z=(\rho)^{5}\cdot(S)^{0.44}\cdot(K) \quad (4)$$

where ρ is relative density of large particles to small and S is the size ratio

$$e=1.53m \quad (5)$$

Therefore, in a generalized format, by incorporating Eq. (4) and (5) in Eq. (3) we get:

$$x=(\rho)^{5}\cdot(S)^{0.44}\cdot(K)\cdot(t)^{1.53m} \quad (6)$$

Factors affecting the attrition rate and attrition phenomena of single particle systems have been extensively studied [18-20]. Apparently, large particles did not take part in the attrition; therefore, only certain material and physical properties were effecting attrition. To gain more insight into the attrition and collision impact mechanism, all samples were evaluated using SEM before and after the attrition test. The catalyst particles morphological analysis suggests that both abrasion and fracturing took place [5]. In fracturing, the size of the particles was largely reduced by breaking into daughter particles, and the process was closely related to severe operating conditions, e.g., high stress [13], number of collusions, etc. In abrasion, the removal of particle edges generates fines and normally the abrasion

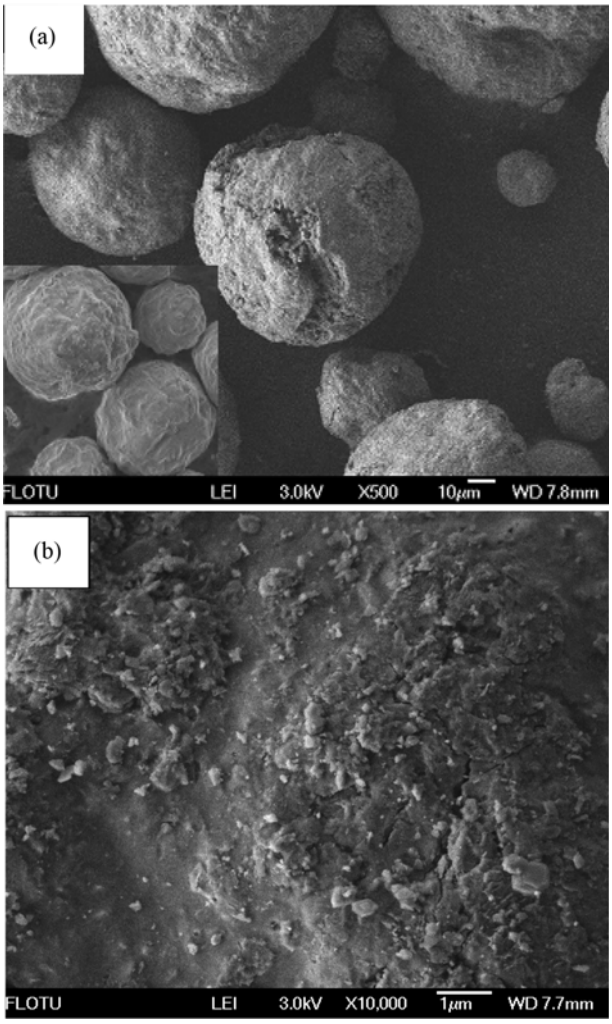

Fig. 7. SEM micrograph of small ZSM-5 catalyst particles (initial particle size 0.098 mm) after being co-fluidized with large ZSM-5 particles of 2.7 mm (density 1.68 g/cm^3) indicates (a) particle before attrition was shown in small window and fractures; and (b) close-up of abrasion after the mixed catalyst air jet attrition test.

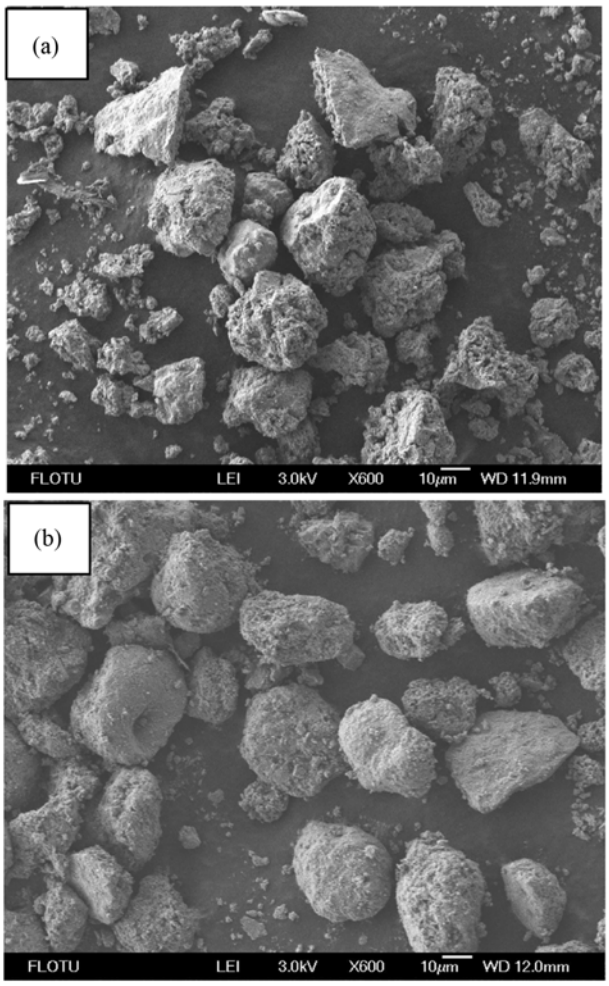

Fig. 8. SEM images after attrition test with hollow ceramic balls of 0.7 mm, density 2.49 g/cm^3 (a) small ZSM-5 particles of 0.098 mm and (b) small SAPO-34 particles of 0.098 mm.

process plays a vital role in fluidized-bed attrition [21,22]. Ghadiri and Zhang studied the impact of single particle on attrition, in controlled loading and proposed a model on the basis of fracturing and chipping phenomena [14]. Salman et al. recently characterized particle fragmentation using a continuous-flow gas gun and successfully developed a numerical model to predict the probability of particle breakage [23].

The attrition phenomena of small particles in a bimodal particles fluidized bed was slightly different from above reported phenomena, because in this system the fracture mechanism plays a vital role in increasing attrition. Moreover, the power of impact was observed to be the function of large particle density and size ratios. Fig. 7 shows that the fractures were appeared on a ZSM-5 particle of 0.098 mm (small particles) during co-fluidization with the same material of size 2.7 mm; the original shape of particles before fluidization was also shown in a small window. Their surface also contains fines of less than 20 μm size generated as a result of further collisions of daughter fragments. These fracturing mechanisms become dominant with respective increase in the density of large particles. The SEM images of Fig. 8 and 9 show the distinct impact of large particles on small particles fragmentation during co-fluidization. Therefore, the small particle attrition during bimodal particle fluidization was due to significant collision impact or shear loads and the hydrodynamic pattern (i.e., because of different densities), those defined the numbers and intensity of collisions. It was observed that independent of the particle sizes, the attrition was reduced by minimizing the relative density difference. Therefore, in sophisticated bimodal (GSS-CFR) with smallest attrition the particles of different sizes should be of the same material.

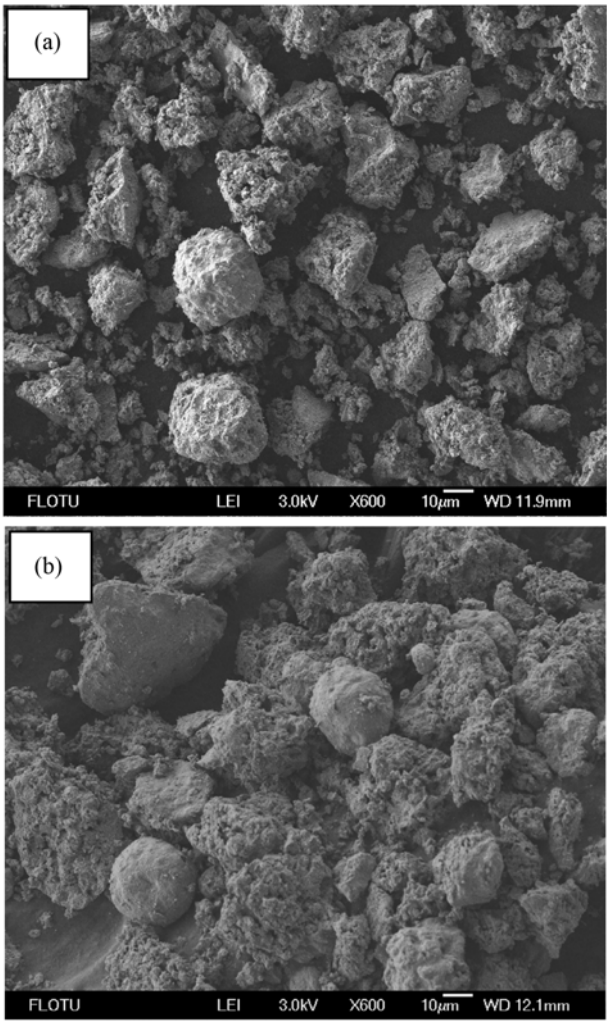

Fig. 9. SEM micrograph after attrition test with ceramic balls of 0.7 mm (density 2.64 g/cm^3) (a) small ZSM-5 particles of 0.098 mm and (b) small SAPO-34 particles of 0.098 mm.

CONCLUSION

ASTM standard air jet fluidized bed test (D-5757) was used to study parameters influencing particle attrition in a bimodal fluidized bed environment. Single particle attrition of each sample was measured in terms of Gwyn constants under identical experimental conditions (single particle system). AJI significantly reflects the overall attrition rate, irrespective of the type of attrition mechanism and is experimentally calculated. Distinct increment in the attrition rate was noted in the case of a bimodal particle fluidization environment (gas-solid-solid system). This increase in attrition rate of small particles was partially influenced by the particle size ratio and largely influenced by the relative density of particles. In addition, significant linear deviation of the Gwyn function was observed during bimodal particle fluidization. The major reason behind this drastic increase in debris (fines) was the distinct fracturing mechanism due to the strong collision impact of large particles on small particles; that was straightforward because of the change in flow regime owing to density variations. A large particle generates higher impact force and peens the surface of small particles. The formulation was designed to measure attrition debris of small particles by defining new constants based on Gwyn constants (which explain small particles' material properties in a bimodal particle fluidization system), relative particle densities and size ratios. Attrition debris of zeolite catalysts (small particles) was calculated from the proposed relationship's simulated results and was compared with the experimental data. The model successfully calculated the attrition debris of catalysts in a bimodal fluidization system; moreover, the narrow span of deviation, i.e., ±0.50 g in attrition debris after 5 hours operation was observed.

ACKNOWLEDGEMENT

This research was supported by the Higher Education Commission, Pakistan (2007PK0013) and Natural Scientific Foundation of China (No. 20606020, No. 20736004, No. 20736007).

NOMENCLATURE

d : particle diameter [mm]
d_T : initial particle diameter [mm]
e : empirical constant
G : exponent characterizing the size distribution
H : hardness [Pa]
K : empirical constant (function of initial particle size)
K_c : fracture toughness [$N \cdot m^{-3/2}$]
l : particle linear dimension [mm]

m : empirical constant
t : time [h]
v : impact velocity
W : mass that has undergone attrition/degradation [g]
W_T : mass degradation product having size less than d_T [g]
X : attrition mass [g]
Z : Zeeshan constant (function of initial particle size)

Greek Letters

α : proportionality constant dimensionless
ξ : fractional loss per impact dimensionless
ρ : relative density, dimensionless
$\acute{\eta}$: dimension less attrition propensity parameter
υ : Poisson ratio dimensionless

REFERENCES

1. Particle Attrition, *British Materials Handling Board. Trans. Tech. Publications*, Germany (1987).
2. D. L. Blair and A. Kudrolli, *Phys. Rev. E.*, **67**, 41301 (2003).
3. J. M. Valverde, A. Castellanos, P. Mills and M. A. S. Quintanilla, *Phys. Rev. E.*, **67**, 51305 (2003).
4. M. J. Pilat and D. S. Ensor, *Atmospheric Environment*, **4**, 163 (1970).
5. J. Bridgwater, R. Utsumi, Z. Zhang and T. Tuladhar, *Chem. Eng. Sci.*, **58**, 4649 (2003).
6. C. R. Bemrose and J. Bridgwater, *Powder Technol*., **49**, 97 (1987).
7. J. E. Gwyn, *AIChE Symposium Series*, **15**, 35 (1969).
8. C. E. Ouwerkerk and D. Ouwerkerk, *Powder Technol*., **65**, 125 (1991).
9. A. U. Neil and J. Bridgwater, *Powder Technol*., **80**, 207 (1994).
10. A. U. Neil and J. Bridgwater, *Powder Technol*., **106**, 37 (1999).
11. C. Crutchley and J. Bridgwater, *KONA Powder and Particle*, **15**, 21 (1997).
12. M. Ghadiri, Z. Ning, S. J. Kenter and E. Puik, *Chem. Eng. Sci.*, **55**, 5445 (2000).
13. A. V. Potapov and C. S. Campbell, *Powder Technol*., **120**, 164 (2001).
14. M. Ghadiri and Z. Zhang, *Chem. Eng. Sci*., **57**, 3659 (2002).
15. K. Johnsen and J. R. Grace, *Powder Technol*., **173**, 200 (2007).
16. ASTM Standard D-5757-Revised, ASTM, Philadelphia PA (2006).
17. R. Boerefijn, N. J. Gudde and M. Ghadiri, *Adv. Powder Technol*., **11**, 145 (2000).
18. H. Kalman, *Powder Technol*., **112**, 244 (2000).
19. J. P. K. Seville, M.A. Mullier, L. Hailu and M. J. Adams, *Fluidization VII*, 586 (1994).
20. M. A. Mullier, J. P. K. Seville and M. J. Adams, *Powder Technol*., **65**, 321 (1991).
21. R. Zhao, J. Goodwin and R. Oukaci, *Appl. Catal. A*., **189**, 99 (1999).
22. S. A. Weeks and P. Dumbill, *Oil Gas J*., **88**, 38 (1990).
23. A. D. Salman, M. J. Hounslow and A. Verba, *Powder Technol.*, **126**, 109 (2002).